



Synthesis of poly(arylene ether sulfone)s with locally and densely sulfonated pentiptycene pendants as highly conductive polymer electrolyte membranes

Feixiang Gong^{a,b}, Suobo Zhang^{a,*}

^a Key Laboratory of Polymer Ecomaterials, Changchun Institute of Applied Chemistry, Chinese Academy of Sciences, Changchun 130022, China

^b Graduate School of Chinese Academy of Sciences, Beijing 100049, China

ARTICLE INFO

Article history:

Received 3 May 2011

Received in revised form 11 July 2011

Accepted 4 August 2011

Available online 11 August 2011

Keywords:

Sulfonated pentiptycene groups

Proton exchange membrane

Low humidity

ABSTRACT

Poly(aryl ether sulfone)s containing sulfonated pentiptycene groups SPES-*x*-PPD are firstly synthesized through nucleophilic aromatic substitution polycondensation by using pentiptycene-6,13-diol, bis(4-hydroxyphenyl) sulfone and 4,4'-difluorodiphenyl sulfone, followed by postsulfonation with concentrated sulfuric acid at room temperature. The structures of SPES-*x*-PPD are characterized by IR, ¹H NMR and ¹³C NMR spectra. These ionomers generally show high thermal stability. Transmission electron microscopic observations reveal that SPES-*x*-PPD membranes form well-defined microphase separated structures. SPES-40-PPD with the IEC value 2.36 mmol g⁻¹ shows conductivity of 2.6 × 10⁻¹ S cm⁻¹ which is much higher than that of perfluorinated Nafion 117 membrane (1.1 × 10⁻¹ S cm⁻¹) at 80 °C and 94% RH. At 80 °C and 34% RH, SPES-40-PPD membrane displays the conductivity of 2.7 × 10⁻³ S cm⁻¹ which is comparable with that of Nafion 117 membrane (3.0 × 10⁻³ S cm⁻¹).

© 2011 Elsevier B.V. All rights reserved.

1. Introduction

Fuel cells (FCs), which convert chemical energy stored in a fuel directly into electricity, are regarded as promising future power sources owing to their advantages, such as high efficiency, high energy density, quiet operation and environmental friendliness [1,2]. Within a fuel cell, the polymer electrolyte membrane serve as an ion conducting and electronically insulating polymer material, is a central, and often performance-limiting, component of the fuel cell [3]. Perfluorinated sulfonic acidic polymers, such as Nafion, have dominated the field because of their excellent chemical and mechanical stabilities as well as high proton conductivity [4,5]. However, there are still some drawbacks of using Nafion including high cost, low operation temperature and high fuel permeability [6]. Hence, in the past decade, a variety of proton exchange membrane (PEM) materials, especially the nonfluorinated aromatic hydrocarbon ionomers, such as poly(phenylene)s, poly(ether ether ketone)s, poly(ether sulfone)s and polyimides have been developed as capable candidates [7–17]. In general, the aromatic hydrocarbon ionomers surpass Nafion in themes of thermal stability, cost, ease of synthesis, and structural diversity. However, their proton conductivity especially under low relative humidity (RH) is still inferior to that of Nafion [18].

Proton conductivity of PEMs is closely related to the acidity of ionic groups and membrane morphology. It is widely recognized that the superior proton conductivity of Nafion is attributed to the strong acidity of –CF₂SO₃H groups and extensive nanoscale phase separation of ionic and nonionic domains [19]. As for aromatic hydrocarbon PEM materials, most of the synthetic methods result in random or statistical disposition of sulfonic acid groups along the hydrophobic polymeric chains. Kreuer have reported that these polymers showed less pronounced nanophase separation morphology and more dead-end channels than that of Nafion [20]. On the other hand, according to previous reports, side-chain-type sulfonated polymers accomplished high proton conductivity due to the distinct phase separation morphology between hydrophilic sulfonic acid side chains and the hydrophobic polymer main chain [18,21,22]. For example, Watanabe et al. reported poly(arylene ether sulfone) based ionomers containing sulfofluorenyl groups [18]. The membranes showed comparable proton conductivity to that of the perfluorinated ionomer membrane (Nafion 112) under a wide range of conditions (80–120 °C and 20–93% relative humidity (RH)). The highest proton conductivity of 0.3 S cm⁻¹ was obtained at 80 °C and 93% relative humidity. Guiver and Jiang et al. reported several aromatic poly(ether ketone)s with pendant sulfonic acid phenyl groups, and they also indicated that polymers with the sulfonated groups attached to pendant side groups are high proton conductive and very stable under heat, hydrolysis and oxidation [23,24]. More recently, it has been found by Ueda that locally and densely sulfonated random copolymers form hydrophilic/hydrophobic phase-separated structures and show

* Corresponding author. Tel.: +86 431 85262118; fax: +86 431 85685653.
E-mail address: sbzhang@ciac.jl.cn (S. Zhang).

high proton conductivity under low humidity conditions [25]. They indicate that high contrast in polarity between hydrophilic and hydrophobic units enables the formation of effective proton paths even in a random copolymer system. Hay et al. prepared sulfonated poly(aryl ether) containing randomly distributed nanoclusters of six or 12 sulfonic acid groups [26]. They found the morphological structure of the copolymers to be comparable to that of Nafion 117.

For the design and preparation of either side-chain or locally and densely sulfonated copolymers, the choice of suitable monomers is crucial. In this study, pentiptycene-6,13-diol is chosen as one of the monomers to produce poly(arylene ether sulfone)s containing pentiptycene groups. After post sulfonation, the four sulfonic acid groups are introduced in pendant side phenyl groups in the each pentiptycene unit. It is expected that such sulfonated copolymers with pendent and locally and densely distributed sulfonic acid groups favor to form hydrophilic and hydrophobic microphase separated structure and high proton conductivity.

2. Experiment

2.1. Materials

Triptycene-1,4-quinone was synthesized according to the literature [27]. Anthracene, quinine, and hydrobromic acid (40%) were purchased from China National Pharmaceutical Group Corporation and used as received. Bis(4-hydroxyphenyl) sulfone (BHPS) (Alfa Aesar), 4,4'-difluorodiphenyl sulfone (DFDPS) (Alfa Aesar) and anhydrous potassium carbonate (Beijing Multi. Technology Co., Ltd.) were used as received without further purification. N-methylpyrrolidone (NMP) was distilled over CaH₂ under reduced pressure. All other reagents were obtained from commercial sources and used as received.

2.2. Synthesis of pentiptycene-6,13-diol

A mixture of anthracene (17.8 g), triptycene-1,4-quinone (28.4 g) and toluene (150 mL) in a 250-mL flask was heated to reflux for 6 h and then cooled to room temperature. The precipitated solid was collected, thoroughly washed with toluene and then dried in vacuum to afford the compound 1 (40.2 g, yield: 87%). To a 500-mL flask, 40.2 g of compound 1 and 350 mL of glacial were charged. The solid was completely dissolved under reflux, then 1 mL of 40% hydrobromic acid was slowly added at the reflux temperature and the mixture was stirred at this temperature for another half hour. After cooling, the white precipitate was filtered, washed with glacial acetic acid and dried in vacuum. The product (compound 2) was obtained in a yield of 85% (34.2 g).

2.3. Synthesis of poly(aryl ether sulfone)s containing pentiptycene groups

The synthesis of the poly(aryl ether sulfone)s containing pentiptycene groups was accomplished by nucleophilic aromatic substitution polycondensation. A typical synthetic procedure, illustrated by the preparation of PES-30-PPD copolymer (30 refers to molar percentage of PPD), is described as follows: 1.3876 g (3 mmol) PPD, 1.7519 g (7 mmol) BHPS, 2.5425 g (10 mmol) DFDPS and 4.1463 g (30 mmol) K₂CO₃ were added into a 100 mL three-neck flask equipped with a magnetic stirrer, a Dean-Stark trap and a nitrogen inlet. Then, 14 mL NMP and 20 mL toluene were charged into the reaction flask under a nitrogen atmosphere. The reaction mixture was refluxed at 140 °C for 4 h until water was removed from the reaction mixture by azeotropic distillation, and then excess toluene was distilled off. Then the mixture was stirred at this temperature for another 10 h to give a viscous solution. The mixture was cooled to 120 °C and diluted with NMP. The solution

was filtered and poured into water to give white flakes of the product, which were washed with hot water several times. The resulting product was dried under vacuum at 120 °C for 12 h. The yield of PES-30-PPD is 98%.

2.4. Sulfonation

The sulfonation reaction was conducted according to the literature method [8]. A typical reaction was shown as follows: to a 100 mL flask, 1 g of PES-30-PPD and 20 mL of concentrated sulfuric acid (98%) were added. After stirring at room temperature for 6 h, the homogeneous viscous solution was poured into a mixture of water and ice to get a silk-like solid. The solid was washed with water until the pH value of water reached neutral. Then the sulfonated copolymer was dried in a vacuum oven at 100 °C for 12 h.

2.5. Membrane preparation

The sulfonated copolymers were cast onto glass plate from their DMAc solution (7–9 wt%) after filtration and dried at 80 °C for 5 h. Then the ionomer membrane was dried in a vacuum oven at 60 °C for 5 h. The as-cast membranes were treated with 1.0 mol L⁻¹ sulfuric acid at room temperature for 2 days for proton exchange. The obtained membranes were thoroughly washed with deionized water. Tough, ductile ionomer membranes were prepared with a controlled thickness of 30–60 μm.

2.6. Measurements

¹H NMR spectra were measured at 300 MHz on a Bruker AV300 spectrometer (Germany). FT-IR spectra of PES-60-PPD and SPES-60-PPD were obtained with a Bio-Rad digilab Division FTS-80 FT-IR spectrometer (Cambridge, MA). The inherent viscosities were determined on 0.5 g dL⁻¹ concentration of polymer in NMP with an Ubbelohde capillary viscometer at 30 ± 0.1 °C. Molecular weight and molecular weight distributions were measured by GPC using Ultrastaygel columns and THF as the eluent at a flow rate of 1 mL min⁻¹. The values obtained were determined by comparison with a series of polystyrene standards. The thermogravimetric analyses (TGAs) were obtained in nitrogen with a Perkin-Elmer TGA-2 thermogravimetric analyzer (Inspiritech 2000 Ltd., UK) at a heating rate of 10 °C min⁻¹. Tensile measurements were performed with a mechanical tester Instron-1211 instrument (Instron Co., USA) at a speed of 2 mm min⁻¹ at 60% relative humidity.

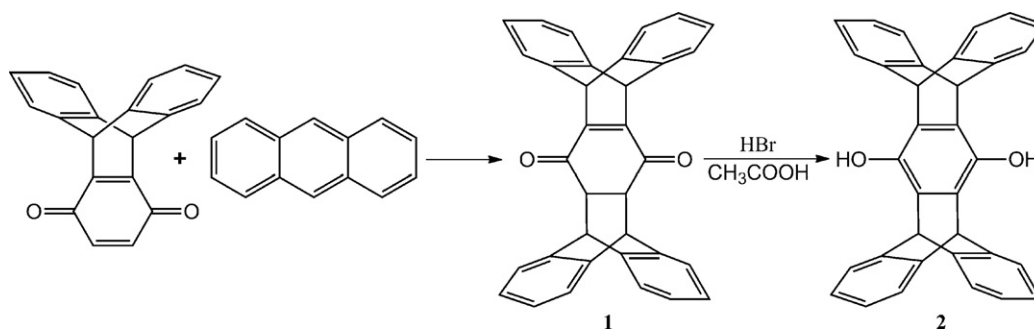
2.7. Ion exchange capacity

IEC of all ionomers were determined by ¹H NMR spectra and titration. In the ¹H NMR method, changes in the integration ratio for the aromatic protons were taken. In the titration method, the membranes in H⁺ form were immersed in a 1 M NaCl solution for 48 h to liberate the H⁺ ions and replace them with Na⁺ ions. The H⁺ ions in solution were then titrated with 0.01 M NaOH aqueous solution and phenolphthalein as the indicator.

2.8. Water uptake and dimensional changes

The humidity dependence of water uptake was measured by placing the membrane in a thermo-controlled humidity chamber for 4 h. Then the membrane was taken out and quickly weighed on a microbalance. Water uptake was calculated from

$$WU (\%) = \frac{W_{\text{wet}} - W_{\text{dry}}}{W_{\text{dry}}} \times 100 \quad (1)$$



Scheme 1. Synthesis of pentiptycene-6,13-diol.

where W_{wet} and W_{dry} are the weights of wet and dried membranes, respectively.

Dimensional change of the hydrated membrane was investigated by plating the membrane in water at 20 °C or 80 °C for 4 h, and the changes of length were calculated from:

$$SR (\%) = \frac{l_{\text{wet}} - l_{\text{dry}}}{l_{\text{dry}}} \times 100 \quad (2)$$

where l_{dry} are the diameter of the dry membrane, l_{wet} refer to those of the hydrated membrane.

2.9. Proton conductivity

The proton conductivity (σ , S cm^{-1}) of each membrane (size: 1 cm \times 4 cm) was obtained using $\sigma = d L_s^{-1} W_s^{-1} R^{-1}$ (d : distance between reference electrodes, and L_s and W_s are the thickness and width of the membrane, respectively). Here, ohmic resistance (R) was measured by four-point probe alternating current (ac) impedance spectroscopy using an electrode system connected with an impedance/gain-phase analyzer (Solatron 1260) and an electrochemical interface (Solatron 1287, Farnborough Hampshire, ONR, UK). The membranes were sandwiched between two pairs of gold-plate electrodes. The membranes and the electrodes were set in a Teflon cell and the distance between the reference electrodes was 1 cm. The cell was placed under a thermocontrolled humid chamber. All samples were equilibrated at the set temperature and humidity for at least 1 h before the measurement.

2.10. Transmission electron microscopy

The membrane samples were stained with lead ions by ion exchange of the sulfonic acid groups in 0.5 M lead acetate aqueous solution, rinsed with deionized water, and dried in vacuum oven for 12 h. Then the dyed sample was embedded in epoxy resin and sectioned using a microtome to yield a 90 nm thick sample which was placed on copper grids. Images were taken on an ultrahigh-resolution transmission electron microscope (JEOLJEM-2010FEF) using an accelerating voltage of 200 kV.

3. Results and discussion

3.1. Synthesis and characterization of monomer and copolymers

The synthetic route for monomer 2 is shown in Scheme 1. Pentiptycene-6,13-diol (PPD) was easily synthesized by two step reactions. First, Diels-Alder reaction of triptycene-1,4-quinone and anthracene formed a compound 1. The subsequent rearrangement reaction using HBr as catalyst afforded high yield diphenol (monomer 2). The proposed structure of target monomer 2 was confirmed by ^1H NMR spectra as shown in Fig. 1. The ^1H NMR data were consistent with the assigned structure of the monomer.

Poly(arylene ether sulfone)s containing pentiptycene groups PES- x -PPD (x refers to molar percentage of PPD) were prepared from PPD, BHPS, and DFDPs (Scheme 2). In a typical procedure for the synthesis of PES- x -PPD, a stoichiometric ratio of PPD-PHPS and DFDPs, an excess of potassium carbonate, and NMP and toluene were used. The reaction was first held at 140 °C for 4 h under nitrogen to remove water by azeotropic distillation and then was stirred at this temperature for another 10 h to afford a high-molecular-weight polymer. All of the PES- x -PPD copolymers showed high molecular weight ($M_n > 69 \times 10^3$ kDa), as evidenced by GPC analyses and their viscosity values (Table 1). The sulfonation of PES- x -PPD copolymers was conducted at room temperature by using concentrated sulfuric acid as both solvents and sulfonating reagent. It was found that all of the sulfonation reaction was completely in 4 h. The degree of sulfonation of the copolymer was readily controlled through the monomer feed ratios of PPD and BHPS. The sulfonated copolymers as synthesized were denoted as SPES- x -PPD. All of the sulfonated copolymers are easily soluble in polar aprotic solvents such as DMAc, DMF and DMSO. Flexible, tough and ductile membranes could be obtained from these sulfonated copolymers by solvent-casting method.

3.2. Characterization of copolymers

Fig. 2 shows the FT-IR spectra of PES-40-PPD and SPES-40-PPD. From the difference between the two curves, it was obvious to see that the symmetric and asymmetric vibrations of the sulfonic acid group appeared at 1165 and 1025 cm^{-1} , respectively. The ^1H NMR (a) and ^{13}C NMR (b) spectra of SPES-40-PPD in DMSO-d_6 are displayed in Fig. 3. Aromatic protons (H_4 , H_7) at the ortho position of the electron donating groups appeared at high field (7.5–6.8 ppm) area while H_5 , H_6 , and H_9 at the ortho position of the electron

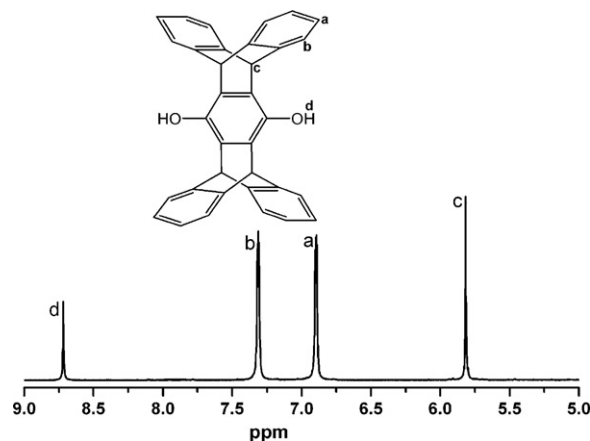


Fig. 1. The ^1H NMR spectra of PPD in DMSO-d_6 .

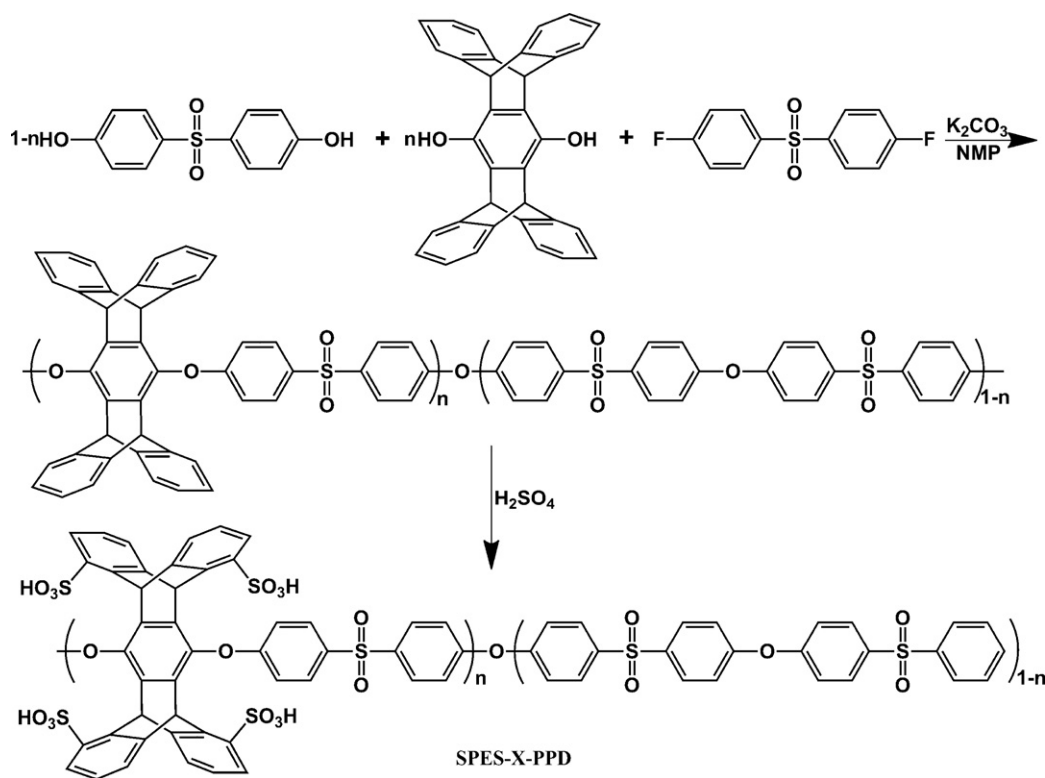
Scheme 2. Synthesis of SPES-*x*-PPD copolymers.

Table 1
Physical properties of PES-*x*-PPD and SPES-*x*-PPD copolymers.

Polymer	PPD (mmol)	BHPS (mmol)	DFDPS (mmol)	Molecular weight (kDa)		η_{inh}^a (dL g ⁻¹)	η_{inh}^b (dL g ⁻¹)
				Mn	PDI		
PES-20-PPD	2	8	10	69	1.49	0.45	0.69
PES-25-PPD	2.5	7.5	10	75	1.56	0.49	0.73
PES-30-PPD	3	7	10	79	1.31	0.51	0.79
PES-35-PPD	3.5	6.5	10	85	1.30	0.54	0.86
PES-40-PPD	4	6	10	89	1.43	0.55	0.91

^a Viscosity before sulfonation; 0.5 g dL⁻¹ in NMP solution at 30 °C.

^b Viscosity after sulfonation; 0.5 g dL⁻¹ in NMP solution at 30 °C.

withdrawing sulfone groups were at low field (8.3–7.8 ppm) area. The protons located at sulfonated pentaerythritol groups were deshielded due to the strongly electron-withdrawing effects of -SO₃H, and their signals transferred into low field area. Meanwhile,

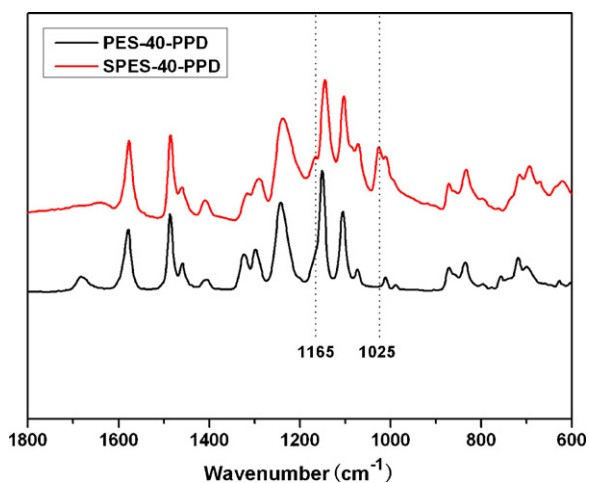


Fig. 2. The IR spectra of PES-40-PPD and SPES-40-PPD.

due to the isomerism of sulfonated pentaerythritol groups as shown in Fig 3(a), the peaks consistent with the protons (carbons) in or next to sulfonated pentaerythritol groups all split into multi-peaks. Combined with the results of ¹³C NMR spectra (Fig. 3(b)), the sites of -SO₃H were readily assigned. No partial sulfonated copolymer peaks could be observed in both ¹H NMR and ¹³C NMR spectra, which suggested that the sulfonation reaction was complete. For all copolymers, the IEC values were calculated from the peak area ratio 9+6+5 to 1+2+3+4+8+7, and the obtained experimental IEC values were in agreement with the expected values from the copolymer composition.

3.3. Thermal and mechanical properties

The thermal stability of the SPES-*x*-PPD copolymers was investigated by thermogravimetric analysis (TGA) in a nitrogen atmosphere as shown in Fig. 4. It can be seen that the SPES-*x*-PPD membranes exhibited a typical three-step degradation pattern. The first weight loss up to 100 °C was ascribed to the loss of water molecules, absorbed by the highly hygroscopic -SO₃H groups. The second weight loss around 350 °C was due to the cleavage of the sulfonic acid groups. The third stage weight loss around 500 °C was assigned the decomposition of polymer main chain. It is con-

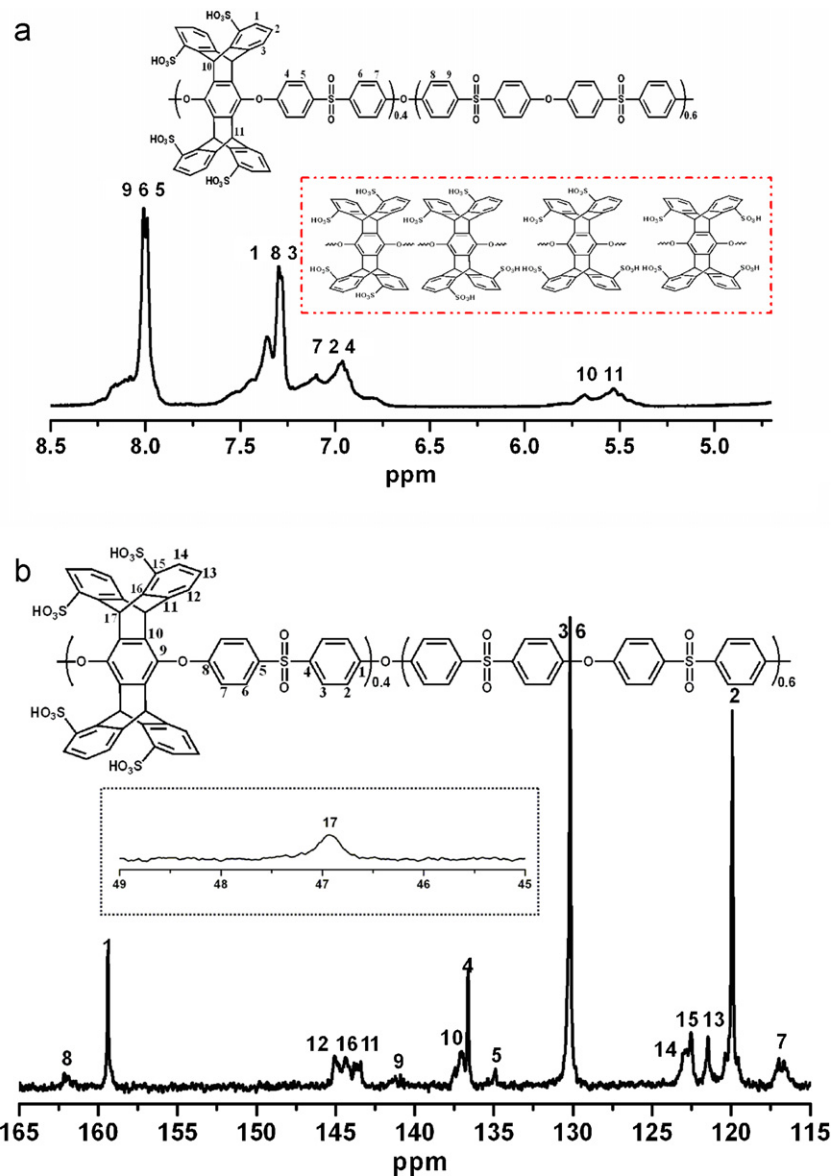


Fig. 3. ¹H (a) and ¹³C NMR (b) spectra of SPES-40-PPD in DMSO-d₆.

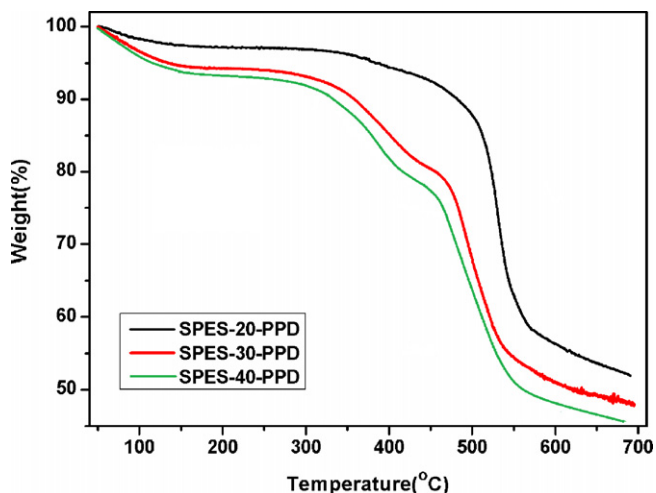


Fig. 4. The TGA curves of SPES-x-PPD copolymers.

cluded that the SPES-x-PPD were thermally stable to satisfy the requirement of thermal stability for the use in PEMFCs.

The mechanical properties of the SPES-x-PPD membranes were measured at room temperature and 60% RH. The stress-strain data are shown in Table 2. The membranes have tensile stress at maximum load of 15.7–44.1 MPa and elongation at break of 3.8–56% with the general trend of lower maximum stress for the higher IEC membranes.

3.4. Water uptake and dimensional changes

Water uptake of membranes is an important factor for proton conductivity because water molecules play an important role as proton transportation carriers in membranes. However, excessive water uptake induces unacceptable dimensional changes and a decrease in the mechanical property. The water uptake data of SPES-x-PPD/SPES-x-PPD membranes are reported in Table 3. As expected, an increase in IEC and temperature led to an increase in water uptake. SPES-40-PPD membrane with highest IEC value

Table 2
IEC and mechanical properties of SPES-*x*-PPD membranes.

Polymer	IEC (mmol g ⁻¹)			Maximum of stress (MPa) ^c	Elongation at break (%)	Young's modulus (MPa)
	IEC _{CAL}	IEC _N ^a	IEC _T ^b			
SPES-20-PPD	1.40	1.36	1.38	44.1	3.8	1160
SPES-25-PPD	1.67	1.65	1.67	34.6	17	739
SPES-30-PPD	1.92	1.89	1.90	28.1	25	588
SPES-35-PPD	2.15	2.17	2.13	25.3	34	476
SPES-40-PPD	2.36	2.35	2.35	15.7	56	219

^a IEC from ¹H NMR spectra.

^b IEC from titration.

^c Measured at room temperature and 60% RH.

Table 3
Water uptake, λ value, swelling ratio and conductivity of SPES-*x*-PPD copolymers.

Polymer	IEC (mmol g ⁻¹)	λ (94% RH)	Water uptake (%) ^a		Swelling ratio (%)		Conductivity (S cm ⁻¹) ^a	
			34% RH	94% RH	Δl^b	Δl^c	34% RH	94% RH
SPES-20-PPD	1.40	6.2	7.6	15.6	5.3	6.3	3.0×10^{-4}	6.9×10^{-2}
SPES-25-PPD	1.67	10.6	9.3	31.8	11.8	15.6	4.3×10^{-4}	1.6×10^{-1}
SPES-30-PPD	1.92	11.3	10.9	39.3	13.7	18.8	1.2×10^{-3}	1.85×10^{-1}
SPES-35-PPD	2.15	12.6	12.5	48.7	21.9	30.1	1.9×10^{-3}	2.3×10^{-1}
SPES-40-PPD	2.36	18.5	17.4	78.6	43.6	89.2	2.7×10^{-3}	2.6×10^{-1}
Nafion 117	0.91	7.1	– ^d	11.6	–	–	3.0×10^{-3}	1.1×10^{-1}

^a Measured at 80 °C.

^b Measured at 20 °C in water.

^c Measured at 80 °C in water.

^d – Not measured.

(2.36 mmol g⁻¹) shows the highest water uptake of 78.6% at 80 °C and 94% RH, corresponding to an absorption of 18.5 water molecules per sulfonic acid group (λ). For all samples, water uptake tended to decrease with decreasing relative humidity. Fig. 5 shows the water uptake as a function of IEC for the SPES-*x*-PPD membranes at 80 °C, 94% and 34% RH, respectively. It can be seen from it that the water uptake showed less dependence with IEC values at low humidity but a great dependence with the IEC values at high humidity. The dimensional changes of SPES-*x*-PPD membranes were evaluated by comparing their hydrated state with dry state at 80 °C and 20 °C, respectively (Fig. 6). As expected, the dimensional changes of SPES-*x*-PPD membranes were in same trend with water uptake. For low IEC membranes, the swelling ratio increased mildly with increasing IEC value. For instance, as shown in Table 3, SPES-25-PPD membrane displayed similar swelling

ratio with SPES-30-PPD membrane at both 20 °C and 80 °C. But the membranes with high sulfonation degree (IEC = 2.36 mmol g⁻¹) exhibited a sharp increase in swelling ratio at both 80 °C (89.2%) and 20 °C (43.6%), attributed to the high water uptake of this membrane. The sharp increase in swelling ratio of SPES-40-PPD membrane would suggest that the IEC value of 2.36 mmol g⁻¹ is a critical value for SPES-*x*-PPD copolymers. Meanwhile, although the swelling ratios of SPES-*x*-PPD membranes were higher than that of Nafion 117 at similar conditions, compared with previously reported copolymers with comparable IEC values, SPES-*x*-PPD membranes had lower dimensional swelling ratios, especially at evaluated temperature [6,28]. This may be attributed that the sulfonic acid groups were fixed in rigid pentiptycene pendants and far away from hydrophobic polymer main chains which makes polymer main chains less susceptible to water swelling.

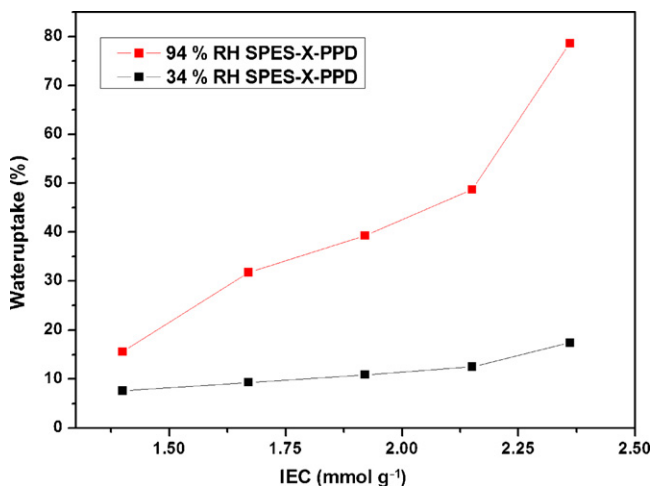


Fig. 5. Water uptake of SPES-*x*-PPD membranes at 80 °C.

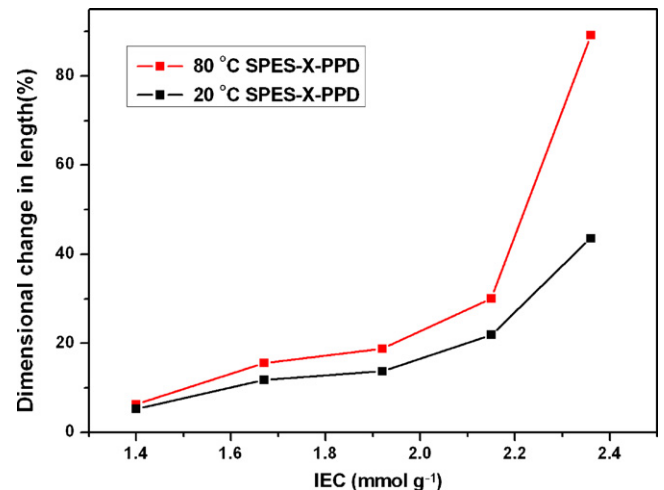


Fig. 6. Swelling ratio of SPES-*x*-PPD membranes at 20 °C and 80 °C in water.

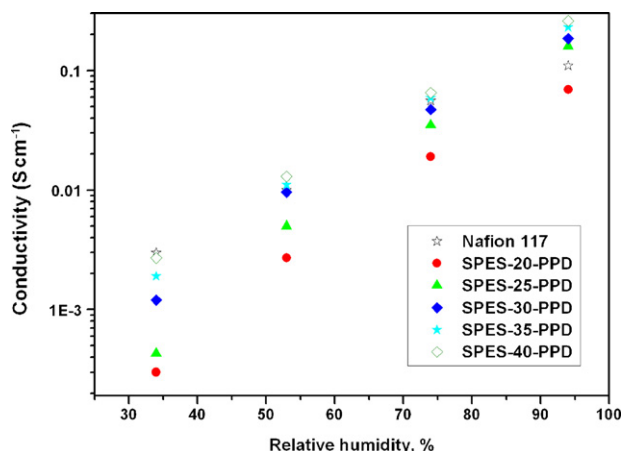


Fig. 7. Humidity dependence of the proton conductivity of SPES-*x*-PPD and Nafion 117 membranes at 80 °C.

3.5. Proton conductivity

The proton conductivities of SPES-*x*-PPD membranes along with that of Nafion 117 were measured at 80 °C in the range of 34–94% RH. As shown in Table 3, SPES-*x*-PPD membranes showed the proton conductivities in the range of 6.9×10^{-2} to 2.6×10^{-1} S cm⁻¹ at 94% RH and 3.0×10^{-4} to 2.7×10^{-3} S cm⁻¹ at 34% RH. As expected, their proton conductivities increased with IEC and water uptake. In order to illustrate the relationship between RH and proton conductivity more clearly, humidity dependence of the proton conductivity of SPES-*x*-PPD and Nafion 117 membranes are also summarized in Fig. 7. It can be seen that the conductivity was low and showed great dependence on humidity for low IEC membranes. For example, the conductivity of SPES-20-PPD (IEC = 1.4 mmol g⁻¹) dropped from 6.9×10^{-2} S cm⁻¹ (94% RH) to 3.0×10^{-4} S cm⁻¹ (34% RH) at 80 °C. This is typical behavior for hydrocarbon ionomer membranes. However, compared with poly(arylene ether sulfone)s containing sulfofluorenyl groups with the similar IEC value [18], the conductivity of SPES-20-PPD membranes was much higher in

a wide range of humidity. This higher conductivity at low humidity was possible due to its better phase separated structures. The higher IEC (IEC > 1.67 mmol g⁻¹) ionomers showed higher or similar proton conductivity in comparison to that of Nafion 117 over a wide humidity range at 80 °C. For example, the SPES-40-TPD membrane with the highest IEC of 2.36 mmol g⁻¹ shows a proton conductivity of 2.6×10^{-1} S cm⁻¹ which is much higher than that of the per-fluorinated Nafion membrane (1.1×10^{-1} S cm⁻¹) at 80 °C and 94% RH. At 80 °C and 34% RH, SPES-40-TPD displays the conductivity of 2.7×10^{-3} S cm⁻¹ which is also comparable with that of the Nafion membrane (3.0×10^{-3} S cm⁻¹). The excellent proton conduction of the SPES-*x*-PPD membranes even under moderate IEC value may be explained by the large difference in polarity between the locally and densely sulfonated units and hydrophobic units of the polymers which resulted in the formation of well-defined phase-separated structures.

3.6. Morphologies of membranes

Proton conductivity of the membranes is closely related to their morphology. In order to clarify the hydrophilic/hydrophobic morphologies of SPES-*x*-PPD membranes, transmission electron microscopic observations were carried out as shown in Fig. 8. The dark areas stained with lead ions represent the hydrophilic (ionic) domain and the brighter areas represent the hydrophobic domain. As is clearly seen in Fig. 8, for SPES-20-PPD membrane with the lowest IEC of 1.4 mmol g⁻¹, only small (about 2–3 nm in diameter), dense and uniform ion clusters could be observed (Fig. 8(a)). The higher IEC (1.92 mmol g⁻¹) causes the formation of bigger spheroidal ionic clusters (about 5–10 nm in diameter) and the connectivity of these ionic clusters was significantly improved. For SPES-40-PPD membrane with the highest IEC of 2.36 mmol g⁻¹, the well-defined and uniform ionic channels (about 10 nm) (Fig. 8(c), dark area) were observed. This unique morphology was expected to provide an effective hydronium ions transport through hydrophilic ionic channels of ionomer membranes. Therefore, the high conductivity was obtained. The well-defined phase separated structures of SPES-40-PPD should be caused by relatively high IEC values and the

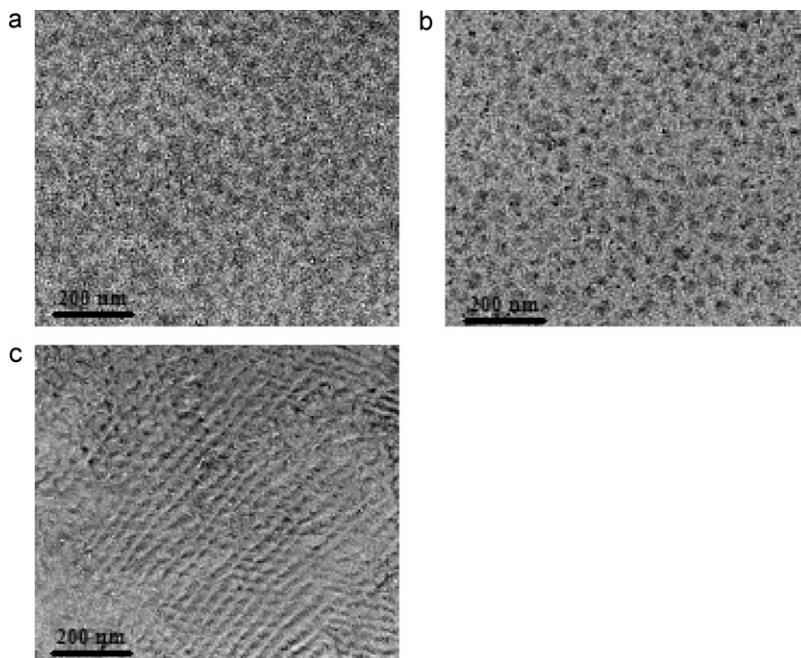


Fig. 8. TEM images of (a) SPES-20-PPD (IEC = 1.4 mmol g⁻¹), (b) SPES-30-PPD (IEC = 1.92 mmol g⁻¹) and (c) SPES-40-PPD (IEC = 2.36 mmol g⁻¹).

large difference in polarity between locally and densely sulfonated units and hydrophobic units of the polymers.

4. Conclusions

Poly(aryl ether sulfone)s containing locally and densely sulfonated pentaerythritol groups SPES-*x*-PPD were easily synthesized through nucleophilic aromatic substitution polycondensation by using pentaerythritol-6,13-diol (PPD), bis(4-hydroxyphenyl) sulfone (BHPS) and 4,4'-difluorodiphenyl sulfone (DFDPS), followed by postsulfonation with concentrated sulfuric acid at room temperature. The sulfonation reaction was easily operated and the degree of sulfonation could be readily and accurately controlled by adjusting the ratio of PPD and BHPS. These ionomers generally show high thermal stability with the degradation temperature of sulfonic acid groups around 350 °C. Meanwhile, due to the large difference in polarity between locally and densely sulfonated units and hydrophobic backbone of the polymers, the well-defined phase separated structures were formed for SPES-*x*-PPD membranes even under moderate IEC value as proved by transmission electron microscopic observations. These novel SPES-*x*-PPD membranes achieved high proton conductivity in a wide range of humidity. In conclusion, the SPES-*x*-PPD membranes should be promising PEM materials especially at high temperature and low humidity.

Acknowledgements

We thank the National Basic Research Program of China (No. 2009CB623401), the National Science Foundation of China (Nos. 50973106, 51021003 and 50825302) for the financial support.

References

- [1] L. Carrette, K.A. Friedrich, U. Stimming, *Fuel Cells* 1 (2001) 5.
- [2] P. Costamagna, S.J. Srinivasan, *J. Power Sources* 102 (2001) 253.
- [3] K.A. Mauritz, R.B. Moore, *Chem. Rev.* 104 (2004) 4535.
- [4] O.J. Savadoga, *New Mater. Electrochem. Syst.* 1 (1998) 47.
- [5] J. Roziere, D.J. Jones, *Annu. Rev. Mater. Res.* 33 (2003) 503.
- [6] M. Hickner, H. Ghassemi, Y. Kim, B. Einsla, J.E. McGrath, *Chem. Rev.* 104 (2004) 4587.
- [7] H. Ghassemi, J.E. McGrath, *Polymer* 45 (2004) 5847.
- [8] B. Liu, G.P. Robertson, M.D. Guiver, W. Hu, Z. Jiang, *Macromolecules* 40 (2007) 1934.
- [9] W.L. Harrison, M.A. Hickner, Y.S. Kim, J.E. McGrath, *Fuel Cells* 5 (2005) 201.
- [10] X. Guo, J. Fang, T. Watari, K. Tanaka, H. Kita, K.I. Okamoto, *Macromolecules* 35 (2002) 6707.
- [11] Z. Qiu, S. Wu, Z. Li, S. Zhang, W. Xing, C. Liu, *Macromolecules* 39 (2006) 6425.
- [12] K. Matsumoto, T. Higashihara, M. Ueda, *Macromolecules* 4 (2008) 7560.
- [13] K. Miyatake, T. Yasuda, M. Hirai, M. Nanasawa, M. Watanabe, *J. Polym. Sci. Part A: Polym. Chem.* 45 (2007) 157.
- [14] B.R. Einsla, Y. Hong, Y.S. Kim, F. Wang, N. Gunduz, J.E. McGrath, *J. Polym. Sci. Part A: Polym. Chem.* 42 (2004) 862.
- [15] Y. Gao, G.P. Robertson, M.D. Guiver, S.D. Mikhailenko, X. Li, S. Kaliaguine, *Macromolecules* 38 (2005) 3237.
- [16] H. Ghassemi, G. Ndip, J.E. McGrath, *Polymer* 45 (2004) 5855.
- [17] X. Glipe, M. Haddad, D.J. Jones, J. Roziere, *Solid State Ionics* 97 (1997) 323.
- [18] K. Miyatake, Y. Chikashige, E. Higuchi, M. Watanabe, *J. Am. Chem. Soc.* 129 (2007) 3879.
- [19] M. Rikukawa, K. Sanui, *Prog. Polym. Sci.* 25 (2000) 1463.
- [20] K.D. Kreuer, *J. Membr. Sci.* 185 (2001) 29.
- [21] B. Lafitte, P. Jannasch, *Adv. Funct. Mater.* 17 (2007) 2823.
- [22] N. Asano, M. Aoki, S. Suzuki, K. Miyatake, H. Uchida, M. Watanabe, *J. Am. Chem. Soc.* 128 (2006) 1762.
- [23] Z. Li, J. Ding, G.P. Robertson, M.D. Guiver, *Macromolecules* 39 (2006) 6990.
- [24] J. Pang, H. Zhang, X. Li, Z. Jiang, *Macromolecules* 40 (2007) 9435.
- [25] K. Matsumoto, T. Higashihara, M. Ueda, *Macromolecules* 42 (2009) 1161.
- [26] S. Matsumura, A.R. Hill, C. Lepiller, J. Gaudet, D. Guay, Z. Shi, S. Holdcroft, A.S. Hay, *Macromolecules* 41 (2008) 281.
- [27] P.D. Bartlett, M.J. Ryan, S.G. Cohen, *J. Am. Chem. Soc.* 64 (1942) 2649.
- [28] P.X. Xing, G.P. Robertson, M.D. Guiver, S.D. Mikhailenko, S. Kaliaguine, *Macromolecules* 37 (2004) 7960.